

Nuclear Model Calculations on the Production of Auger Emitter ^{165}Er for Targeted Radionuclide Therapy

Mahdi Sadeghi¹, Milad Enferadi², Claudio Tenreiro³

¹Agricultural, Medical and Industrial Research School, Nuclear Science and Technology Research Institute, Karaj, Iran

²Faculty of Engineering, Research and Science Campus, Islamic Azad University, Tehran, Iran

³Department of Energy Science Sungkyunkwan University, Suwon, Korea

E-mail: msadeghi@nrcam.org

Received June 6, 2010; revised July 16, 2010; accepted June 25, 2010

Abstract

Auger electron emitting radionuclides have potential for the therapy of small-size cancers because of their high level of cytotoxicity, low-energy, high linear energy transfer, and short range biologic effectiveness. Auger emitter ^{165}Er ($T_{1/2} = 10.3$ h, $I_{\text{EC}} = 100\%$) is a potent nuclide for targeted radionuclide therapy. ^{165}Er excitation function via $^{165}\text{Ho}(p,n)^{165}\text{Er}$, $^{165}\text{Ho}(d,2n)^{165}\text{Er}$, $^{166}\text{Er}(p,2n)^{165}\text{Tm} \rightarrow ^{165}\text{Er}$, $^{166}\text{Er}(d,3n)^{165}\text{Tm} \rightarrow ^{165}\text{Er}$, $^{165}\text{Er}(p,xn)^{165}\text{Tm} \rightarrow ^{165}\text{Er}$ and $^{164}\text{Er}(d,n)^{165}\text{Tm} \rightarrow ^{165}\text{Er}$ reactions were calculated by ALICE/91, ALICE/ASH (GDH Model & Hybrid Model) and TALYS-1.2 (Equilibrium & Pre-Equilibrium) codes and compared to existing data. Requisite for optimal thicknesses of targets were obtained by SRIM code for each reaction.

Keywords: ^{165}Er , Auger Electron, Excitation Functions, TALYS-1.2, ALICE-ASH

1. Introduction

The double strand DNA helix presents a diameter of 2 nm. In a typical Auger radiation decay, the highest energy deposition occurs in spheres of 1-2 nm, as described elsewhere [1]. This means that the calculated local energy deposition of an Auger emitter incorporated into DNA would hit both DNA strands with an energy of 1.6 MGy or higher. This radiation energy is therefore largely sufficient to disrupt both DNA strands over distances of several nucleotides [2,3]. Auger electron emitting radionuclides in cancer therapy offer the opportunity to deliver a high radiation dose to the tumor cells with high radiotoxicity while minimizing toxicity to normal tissue [4]. Besides the direct effect of Auger electrons on DNA double strands, an indirect radiation effect of Auger energy deposition will occur via production of radicals [5]. The radicals diffuse freely in the intracellular space and can cause further DNA damage. Even a bystander effect by diffusion of radicals through gap junctions has been described [6]. Only very few radionuclides exist that decay exclusively by EC-mode without any accompanying radiation, ^{165}Er is one of them. Auger electrons are emitted by isotopes that decay by electron capture (EC) or have internal conversion (IC) in their decay. In each decay of these isotopes, a cascade of very low energy

electrons is emitted [7].

In this work, several methods for ^{165}Er production using ALICE/91, ALICE/ASH (GDH Model & Hybrid Model) and TALYS-1.2 (Equilibrium & Pre-Equilibrium) codes have been studied. Aim of the presented study is to compare the calculated cross sections for the production of ^{165}Er via different reactions with incident particle energy up to 50 MeV as a part of systematic studies on particle-induced activations on metal targets, theoretical calculation of production yield, calculation of target thickness requirement and suggestion for optimum reaction to produce Erbium-165.

2. Theory

2.1. Calculation of Excitation Function

Cross sections for $^{165}\text{Ho} + p, d$, $^{166}\text{Er} + p, d$, $^{164}\text{Er} + d$ and $^{165}\text{Er} + p$ reactions were calculated by using ALICE/91, ALICE/ASH (GDH Model & Hybrid Model) and TALYS-1.2 (Equilibrium & Pre-Equilibrium) codes [9-11]. The codes were used simultaneously to increase the accuracy of calculations. An optimum energy range was determined and employed to avoid the formation of the radionuclide impurities and decrease the excitation functions of the inactive impurities as far as possible. To fur-

ther achieve the aim, feasibility of the ^{165}Er production via various nuclear reactions per low/medium energy accelerators was investigated. According to SRIM code (The Stopping and Range of Ions in Matter); the required thickness of the target was calculated for each reaction.

2.2. ALICE/ASH Code

The ALICE/ASH code [12] is a modified and advanced version of the ALICE code [9] and ALICE/LIVERMORE. The geometry dependent hybrid model (GDH) as adopted originally is used for the description of the pre-equilibrium particle emission from nuclei [13,14].

2.2.1. Pre-Compound Deuteron Emission

Following closely the exhaustive analysis of the code ALICE/ASH by Broeders and its collaborators [12] the main features of the deuteron emission from the compound systems (as a cluster), relative to the Fermi Energy (E_F), from all the reaction channels, are summarized as:

- 1) At energies below the E_F , the pick-up of nucleons,
- 2) At energies above E_F the possible coalescence of

$$\omega(p,h,E) = g^p \tilde{g}^h \sum_{k=0}^h C_k (-1)^k \Theta(E - kE_F) \frac{(E - kE_F)^{n-1}}{p!h!(n-1)!} \quad (2)$$

where E is the excitation energy, E_F is the Fermi energy, g and \tilde{g} are the single particle level densities for particles and holes, respectively, $\Theta(x)$ is the Heaviside function, $\Theta = 0$ for $x < 0$ and $\Theta = 1$ for $x > 0$. The single particle level densities for particles and holes are calculated by Beták and Dobeš [16]

$$g = A/14 \quad (3)$$

$$\frac{d\sigma^{p-U,C}}{d\varepsilon_d} = \sigma_{\text{non}}(E_0) \sum_{n=n_0} \sum_{k+m=2} F_{k,m}(\varepsilon_d + Q_d) \frac{\omega(p-k,h,U)}{\omega(p,h,E)} \frac{\lambda_d^e(\varepsilon_d)}{\lambda_d^e(\varepsilon_d) + \lambda_d^+(\varepsilon_d)} g_d D_n \quad (5)$$

where $F_{k,m}$ is the deuteron formation factor equal to the probability that the deuteron is composed of “ k ” particles above the Fermi level and “ m ” particles below; ε_d is the channel emission energy corresponding to the deuteron emission; λ_d^e is the deuteron emission rate; λ_d^+ is the intranuclear transition rate for the absorption of the deu-

$$\frac{d\sigma^{k-O}}{d\varepsilon_d} = \sigma_{\text{non}}(E_0) \sum_{n=n_0} \Phi_d(E_0) \frac{g}{g_d p} \frac{\omega(p-1,h,U)}{\omega(p,h,E)} \frac{\lambda_d^e(\varepsilon_d)}{\lambda_d^e(\varepsilon_d) + \lambda_d^+(\varepsilon_d)} g_d D(n) \quad (6)$$

teron in the nucleus; g_d is the density of single particle states for the deuteron. The deuteron emission (λ_d^e) and absorption (λ_d^+) rates are calculated. In analogy with α -particle emission the knock-out component of the pre-compound deuteron emission spectrum is written as follows

$$\Phi_d = 2F_d(E_0) \quad (7)$$

where F_d is the probability of interaction of the incident

states of two excited nucleons,

3) The possibility of reactions that includes the Knock-out of a “pre-formed” deuteron

4) Finally the inclusion of a fast or peripheral direct mechanism resulting in deuteron formation and escape.

Taking into consideration all the above, the modified code calculates the deuteron spectrum from the contribution of the individual differential cross sections of such processes as

$$\frac{d\sigma}{d\varepsilon_d} = \frac{d\sigma^{\text{PU,C}}}{d\varepsilon_d} + \frac{d\sigma^{\text{KO}}}{d\varepsilon_d} + \frac{d\sigma^{\text{D}}}{d\varepsilon_d} \quad (1)$$

The upper index stands for Pick-Up, Coalescence, Knock-out and Direct reaction respectively. The cross sections are in somehow proportional to the relative number of states available for such reaction channel to occur. Expressions for such cross sections were derived by Broeders *et al.* [13].

Using basic statements of the hybrid model [15]. The exciton level density is calculated by Beták and Dobeš [23] taking into account the finite depth of the nuclear potential well

$$\tilde{g} = A/E_F \quad (4)$$

One should note that nuclear surface effects [17-19] influence the effective value of the Fermi energy E_F used for the calculation of pre-compound particle spectra. This point is discussed below. The exciton coalescence pick-up model proposed by Sato *et al.* [20] is used for the calculation of the $d\sigma^{\text{P-U,C}}/d\varepsilon_d$ spectrum component [28].

teron in the nucleus; g_d is the density of single particle states for the deuteron. The deuteron emission (λ_d^e) and absorption (λ_d^+) rates are calculated. In analogy with α -particle emission the knock-out component of the pre-compound deuteron emission spectrum is written as follows

particle with the “pre-formed” deuteron resulting in its excitation in the nucleus; and the factor of two reflects the normalization on the number of particles in the initial exciton state n_0 . The general expression for F_d is [21]

$$F_d = \frac{\varphi \sigma_{xd}(E_0)}{\frac{Z'}{A'} \sigma_{xp}(E_0) + \frac{(A' - Z')}{A'} \sigma_{xn}(E_0) + \varphi \sigma_{xd}(E_0)} \quad (8)$$

where “x” refers to the initial proton or neutron, σ_{xd} , σ_{xp} and σ_{xn} are the cross-sections of the elastic interaction of projectile with deuteron, proton and neutron, respectively, corrected for a Pauli principle, φ is the number of “pre-formed” deuterons in the nucleus, Z' and A' are the number of protons and nucleons in the nucleus corrected for a number of clustered deuterons.

The direct component of the deuteron spectrum is [21]

$$\frac{d\sigma^D}{d\varepsilon_d} = \sigma_{\text{non}} \frac{\omega^*(U)}{\omega(1p,0h,E)} \frac{\lambda_d^e(\varepsilon_d)}{\lambda_d^e(\varepsilon_d) + \lambda_d^+(\varepsilon_d)} g_d \quad (9)$$

where the final level density $\omega^*(U)$ is approximated by $\omega(0p,1h,U) \cdot \gamma / g_d$ with the γ value equal to 0.002 MeV^{-1} for all nuclei and excitation energies. To improve the agreement of calculations and the measured deuteron spectra, it is useful to write the direct component of the spectrum in the following form

$$\frac{d\sigma^D}{d\varepsilon_d} = \sigma_{\text{non}} \alpha_1 \exp\left(-\frac{(E - \alpha_2 E_F)^2}{2(\alpha_3 E_F)^2}\right) \frac{\lambda_d^e(\varepsilon_d)}{\lambda_d^e(\varepsilon_d) + \lambda_d^+(\varepsilon_d)} g_d \quad (10)$$

where α_1 , α_2 and α_3 are parameters and E_F is the effective value of the Fermi energy. The values of α_i can be obtained from analysis of experimental deuteron spectra. The global parameterization of α_i parameters is hardly possible [12].

2.3. TALYS-1.2 Code

TALYS-1.2 code is optimized for incident projectile energies, ranging from 1 keV up to 200 MeV on target nuclei with mass numbers between 12 and 339. It includes photon, neutron, proton, deuteron, triton, ^3He , and α -particles as both projectiles and ejectiles, and single-particle as well as multi-particle emissions and fission. All experimental information on nuclear masses, deformation, and low-lying states spectra is considered, whenever available [22] and if not, various local and global input models have been incorporated to represent the nuclear structure properties, optical potentials, level densities, γ -ray strengths, and fission properties. The TALYS code was designed to calculate total and partial cross sections, residual and isomer production cross sections, discrete and continuum γ -ray production cross sections, energy spectra, angular distributions, double differential spectra, as well as recoil cross sections. The pre-equilibrium particle emission is described using the two-component Exciton model. The model implements

new expressions for internal transition rates and new parameterization of the average squared matrix element for the residual interaction obtained using the optical model potential [23,24]. The phenomenological model is used for the description of the pre-equilibrium complex particle emission. The equilibrium particle emission is described using the Hauser-Feshbach formalism.

3. Results

In the calculations of the hybrid and GDH model, the code ALICE/ASH was used. This code can be applied for the calculation of excitation functions, energy and angular distribution of secondary particles in nuclear reactions induced by nucleons and nuclei with energy up to 300 MeV. The generalized superfluid [25] has been applied for nuclear level density calculations in the ALICE/ASH code. The ALICE-91 and ALICE/ASH codes use the initial exciton number as $n_0 = 3$. But in these models the different alpha (α), deuteron (d) and proton (p) exciton numbers are used in the pre-equilibrium GDH model calculations. In details, the other code model parameters can be found in reference [12]. In ALICE/ASH code, the hybrid and geometry dependent hybrid model (GDH) for pre-compound emissions and the Weisskopf-Ewing model for compound reactions are selected.

Although there are some discrepancies between the calculations and the experimental data, in generally, the new evaluated hybrid and GDH the pre-equilibrium model calculations (with ALICE/ASH) are very close to the experimental data in **Figures 1, 2, and 6**. In addition, the GDH and hybrid model calculations are close to each other, generally. Indeed, calculated emission cross sections with GDH and hybrid model by using ALICE/ASH code show the best agreement with the experimental data for $^{165}\text{Er}(p,xn)^{165}\text{Tm} \rightarrow ^{165}\text{Er}$ reaction in **Figure 6**. Moreover, these cross sections in harmony with the experimental data for $^{165}\text{Ho}(p,2n)^{165}\text{Er}$ nuclei except for the (p,n) reaction in which the experimental data have followed above theoretical calculations in **Figure 1**.

The reason is that the new developed pre-equilibrium reaction mechanism ALICE/ASH includes angular momentum conversion. Not only it gives us more information for new nuclear reaction research, but also it lets us calculate cross sections up to many hundreds MeV energy level. In fact, when taking the pairing energy and the mass shell correction into consideration, the experimental values are in better agreement with the theoretical results [26]. In conclusion all figures show that, although a few calculated data follow the experimental ones from above or below as parallel, generally all the compared data are in agreement with each other.

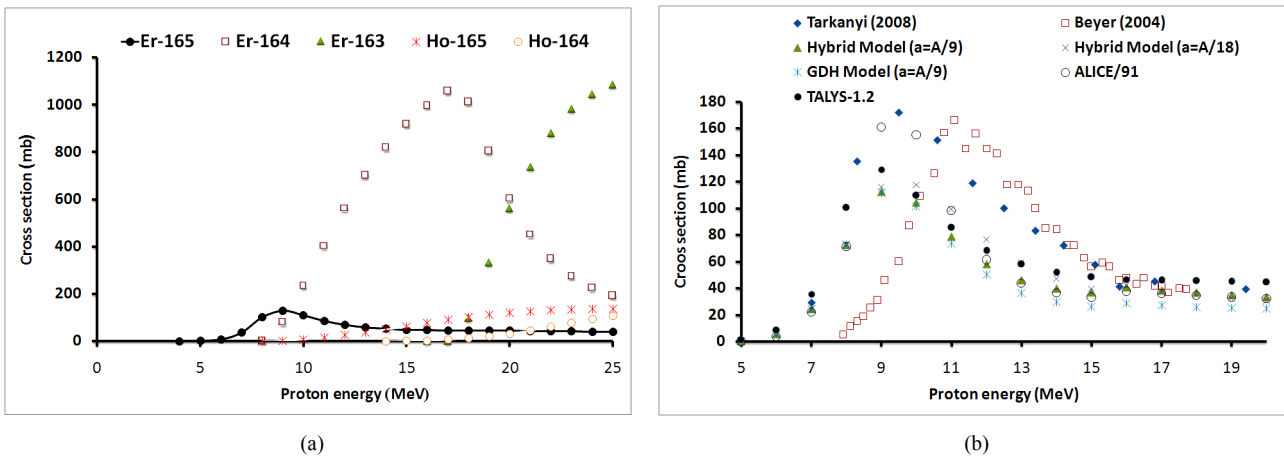


Figure 1. Excitation function of $^{165}\text{Ho}(p,n)^{165}\text{Er}$ reaction by: (a) TALYS 1.2 code (b) comparison of calculated excitation functions of $^{165}\text{Ho}(p,n)^{165}\text{Er}$ reaction with the values reported in literature.

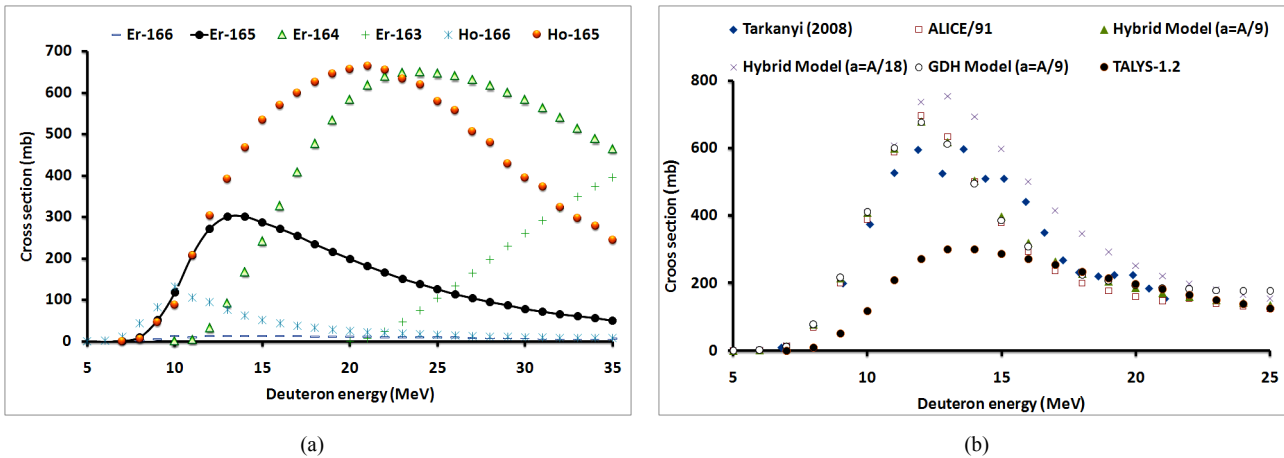


Figure 2. Excitation function of $^{165}\text{Ho}(d,2n)^{165}\text{Er}$ reaction by: (a) TALYS 1.2 code (b) comparison of calculated excitation functions of $^{165}\text{Ho}(d,2n)^{165}\text{Er}$ reaction with the values reported in literature.

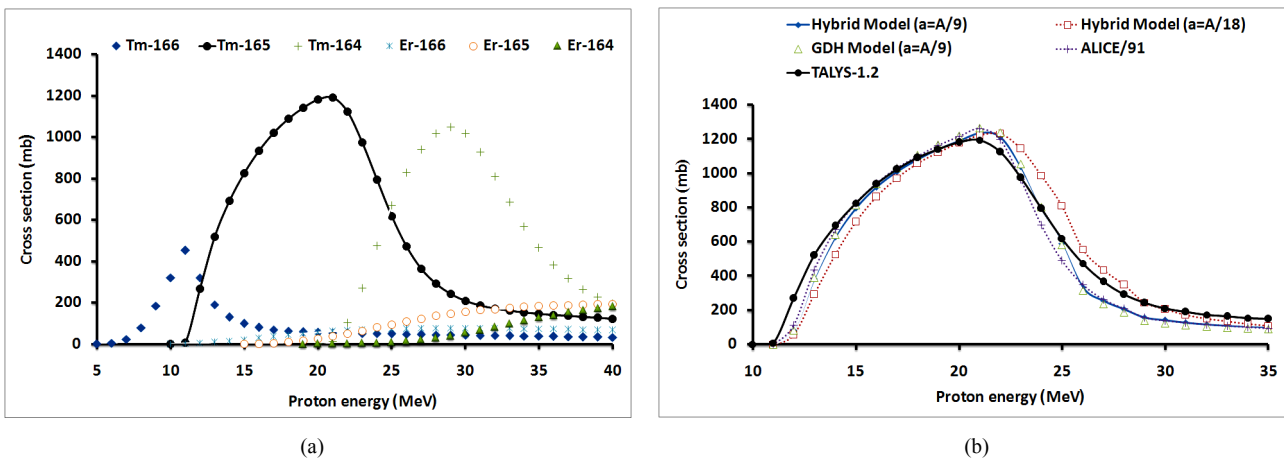


Figure 3. Excitation function of $^{166}\text{Er}(p,2n)^{165}\text{Tm} \rightarrow ^{165}\text{Er}$ reaction by: (a) TALYS 1.2 code (b) codes. No experimental data are reported in literature.

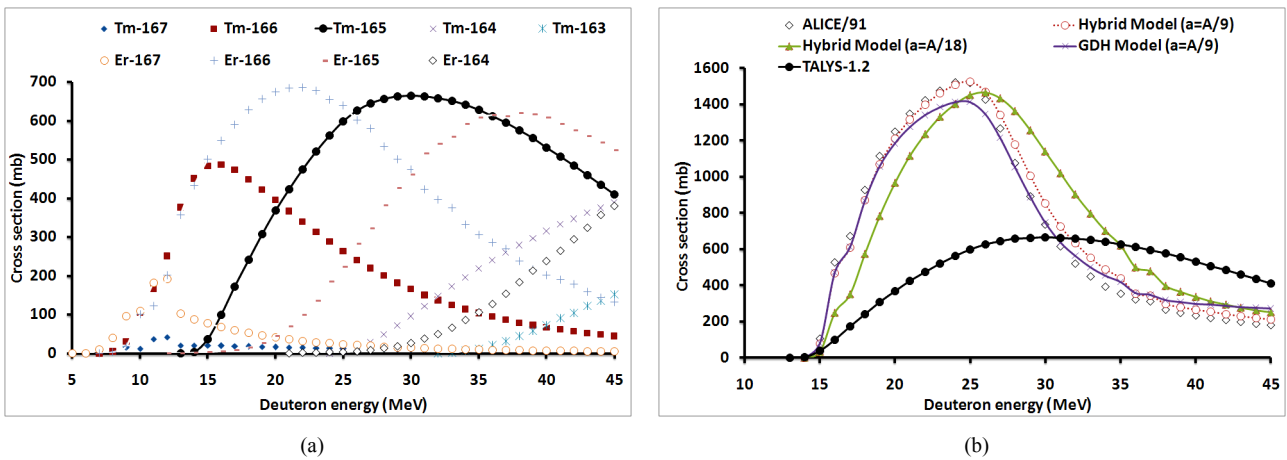


Figure 4. Excitation function of $^{166}\text{Er}(d,3n)^{165}\text{Tm} \rightarrow ^{165}\text{Er}$ reaction by: (a) TALYS 1.2 code (b) other codes. No experimental data are reported in literature.

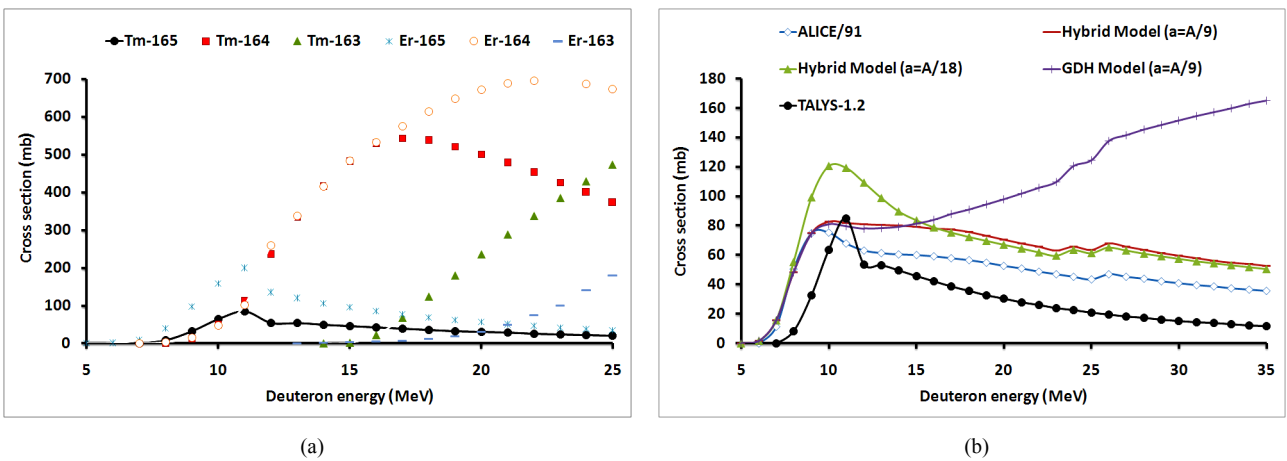


Figure 5. Excitation function of $^{164}\text{Er}(d,n)^{165}\text{Tm} \rightarrow ^{165}\text{Er}$ reaction by: (a) TALYS 1.2 code (b) and other codes. No experimental data are reported in literature.

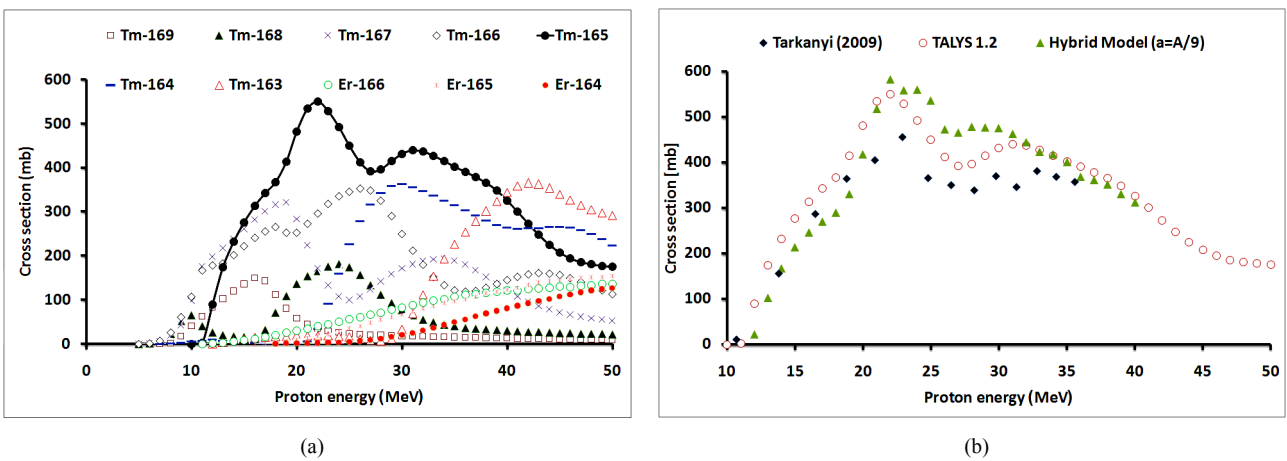


Figure 6. Excitation function of $^{nat}\text{Er}(p,xn)^{165}\text{Tm} \rightarrow ^{165}\text{Er}$ reaction by: (a) TALYS 1.2 code (b) comparison of calculated excitation functions of $^{nat}\text{Er}(p,xn)^{165}\text{Tm} \rightarrow ^{165}\text{Er}$ reaction with the values reported in literature.

3.1. Excitation Function of $^{165}\text{Ho}(p,n)^{165}\text{Er}$ Reaction

Excitation functions of the proton-induced reaction on Holmium-165 were determined by ALICE/91, ALICE/ASH and TALYS-1.2 codes, and the experimental data that have been studied by Beyer *et al.* (2004) [27] and Tárkányi *et al.* (2008) [28]. The evaluation of the results of the calculations showed that the best range of energy that favor the reaction is from 12 to 7 MeV. Carrier-free ^{165}Er production can be obtained using a proton an energy of less than 9 MeV. There is a relatively good agreement between the experimental data by Tárkányi *et al.* and the prediction of the excitation function made by ALICE/91 code up to 11 MeV. According to calculations from SRIM code the required target thickness should be $34.04\ \mu\text{m}$ (See **Figure 1**).

3.2. Excitation Function of $^{165}\text{Ho}(d,2n)^{165}\text{Er}$ Reaction

According to results from the ALICE/91, ALICE/ASH and TALYS-1.2 codes, the optimum energy range for the projectile particle (deuteron) to produce ^{165}Er from ^{165}Ho target in this case is from 16 to 11 MeV. Hybrid Model predicts that the maximum of the cross section ($a = A/18$) is $753.6\ \text{mb}$ at an energy of 13 MeV. The separation of isotope impurities is not possible by chemical methods, so this reaction is non carrier free for ^{165}Er production (See **Figure 2**). This reaction was investigated only by Tárkányi *et al.* (2008) [29]. ALICE/91 and ALICE/ASH codes agree well with the measured data from Tárkányi *et al.* up to 20 MeV. Also, the results of TALYS-1.2 code are less than experimental data, ALICE/91 and ALICE/ASH codes.

3.3. Excitation Function of $^{166}\text{Er}(p,2n)^{165}\text{Tm} \rightarrow ^{165}\text{Er}$ Reaction

^{165}Er can also be produced using the $^{166}\text{Er}(p,2n)^{165}\text{Tm}$ reaction which is unstable, ^{165}Tm ($T_{1/2} = 30.06\ \text{h}$), the best range of incident energy was estimated for proton energies from 23 to 16 MeV. The maximum for the cross section, as by the GDH model ($a = A/9$) is predicted to be $1263.3\ \text{mb}$ at the energy of 21 MeV. Also $^{166/164}\text{Tm}$ impurities are generated which cannot be separated by chemical methods. Also this reaction was leading to non-isotopic impurities of stable ($^{166/164}\text{Er}$). There have not been any experimental data for these reactions in the literature, therefore only theoretical calculations have been shown in **Figure 3**. Also, there is a relatively good agreement between the prediction of the excitation function made by TALYS-1.2, ALICE/91 and ALICE/ASH

codes. The theoretical thick target will give a yield of $107.3\ \text{MBq}/\mu\text{A}\cdot\text{h}$. Recommended thickness of the target is $31.8\ \mu\text{m}$.

3.4. Excitation Function of $^{166}\text{Er}(d,3n)^{165}\text{Tm} \rightarrow ^{165}\text{Er}$ Reaction

According to codes, optimal energy range of the projectile particle (deuteron) to produce ^{165}Tm from ^{166}Er target is from 22 to 29 MeV within this range the maximum cross section predicted by Hybrid Model ($a = A/9$) is $1523.9\ \text{mb}$ at an energy of 25 MeV. Also ^{166}Tm ($T_{1/2} = 7.7\ \text{h}$), ^{164}Tm ($T_{1/2} = 2\ \text{min}$) and ^{163}Tm ($T_{1/2} = 1.81\ \text{h}$) impurities are generated which cannot be separated by chemical methods. The non-isotopic impurities of active ($^{166/165}\text{Er}$) were also produced in the reaction. There have not been any experimental data for these reactions in the literature, therefore only theoretical calculations have been shown in **Figure 4**, so nuclear model calculations can play an important role in excitation function of $^{166}\text{Er}(d,3n)^{165}\text{Tm} \rightarrow ^{165}\text{Er}$ reaction. Also, the results of TALYS-1.2 code are less than ALICE/91 and ALICE/ASH codes. The theoretical thick target gives a yield of $42.9\ \text{MBq}/\mu\text{Ah}$. Recommended thickness of the target is $31.4\ \mu\text{m}$.

3.5. Excitation Function of $^{164}\text{Er}(d,n)^{165}\text{Tm} \rightarrow ^{165}\text{Er}$ Reaction

According to ALICE/91, ALICE/ASH and TALYS-1.2 codes, the best energy range of the projectile particle (Deuteron) to produce ^{165}Tm from ^{164}Er target is found to be from 13 to 8 MeV and maximum cross section is predicted by the Hybrid model ($a = A/18$) to be $120.4\ \text{mb}$ at an energy of 10 MeV. Also ^{164}Tm ($T_{1/2} = 2\ \text{min}$) and ^{163}Tm ($T_{1/2} = 1.81\ \text{h}$) impurities are generated and they could not be separated by chemical methods (See **Figure 5**). This reaction was also producing Non-isotopic impurities of high cross section ($^{164/163}\text{Er}$). The theoretical thick target yield is $0.074\ \text{MBq}/\mu\text{A}\cdot\text{h}$. Recommended thickness of the target is $90\ \mu\text{m}$.

3.6. Excitation Function of $^{nat}\text{Er}(p,xn)^{165}\text{Tm} \rightarrow ^{165}\text{Er}$ Reaction

Excitation functions of the proton-induced reaction on ^{nat}Er were calculated by ALICE/ASH and TALYS-1.2 codes. The data from the calculations showed that in order to optimize isotope production the best range of the energy is 29 to 20 MeV. The calculated excitation functions of $^{nat}\text{Er}(p,xn)^{165}\text{Tm} \rightarrow ^{165}\text{Er}$ reactions are compared with the existing experimental values in **Figure 6**. The results of TALYS-1.2 and ALICE/ASH codes are good

Table 1. ^{165}Er production yield via different nuclear reactions by SRIM and TALYS 1.2 codes.

Reaction	Isotopic abundance (%)	Energy range (MeV)	Target thickness (μm)	Theoretical yield (MBq/ μAh)
$^{165}\text{Ho}(p,n)^{165}\text{Er}$	100	12→7	75	34.04
$^{165}\text{Ho}(d,2n)^{165}\text{Er}$	100	16→11	61	77.7
$^{166}\text{Er}(p,2n)^{165}\text{Tm} \rightarrow ^{165}\text{Er}$	33.6	23→16	31.8	107.3
$^{166}\text{Er}(d,3n)^{165}\text{Tm} \rightarrow ^{165}\text{Er}$	33.6	29→22	31.4	42.9
$^{164}\text{Er}(d,n)^{165}\text{Tm} \rightarrow ^{165}\text{Er}$	1.61	13→8	90	0.074
$^{nat}\text{Er}(p,xn)^{165}\text{Tm} \rightarrow ^{165}\text{Er}$	100	29→20	27.9	210.9

agreement with the measured data from Tárkányi *et al.* (2009) [30]. The separation of isotope impurities is not possible by chemical methods, so this reaction is non carrier free for ^{165}Tm production. According to SRIM code the required target thickness should be 210.9 μm .

3.7. Calculation of the Required Thickness of Target

To obtain the optimum physical dimensions of the target such as the thickness some estimations from the SRIM code (The Stopping and Range of Ions in Matter); were performed [31]. The physical thickness of the target layer is chosen in such a way that, for a given beam/target angle geometry (90°), the incident beam on the target area will produce a compound nucleus with an excitation energy with the calculated optimum energy to favor the selected evaporation channel. To minimize the thickness of the thin film target, a geometry of 6° is preferred; so the required thickness of the layer will be smaller with a coefficient 0.1 (note: it is not clear what this phrase means, what is such coefficient). The calculated thicknesses for these ideal reactions are shown in **Table 1**.

3.8. Calculation of Theoretical Yield

Enhance of the projectile energy, the beam current and the time of bombardment increase the production yield. The production yield can be calculated as below,

$$Y = \frac{N_L H}{M} I (1 - e^{-\lambda t}) \int_{E_1}^{E_2} \left(\frac{dE}{d(\rho x)} \right)^{-1} \sigma(E) dE \quad (11)$$

where Y is the product activity (in Bq) of the product, N_L is the Avogadro number, H is the isotope abundance of the target nuclide, M is the mass number of the target element, $\sigma(E)$ is the cross section at energy E, I is the projectile current, $\frac{dE}{d(\rho x)}$ is the stopping power, λ is

the decay constant of the product and t is the time of irradiation [32]. The production yields of ^{165}Er via different reactions were calculated using the Simpson numerical integral as of Equation (11) (**Table 1**).

4. Conclusions

Result of the calculations and considerations predicted that the high yield will be achieved by deuteron bombardment of a natural erbium target. Nevertheless this processes lead to form the radioisotope and isotope impurities that have high cross section than ^{165}Er . $^{164}\text{Er}(d,n)^{165}\text{Tm} \rightarrow ^{165}\text{Er}$, $^{166}\text{Er}(d,3n)^{165}\text{Tm} \rightarrow ^{165}\text{Er}$ and $^{165}\text{Ho}(d,2n)^{165}\text{Er}$ reactions are too much undesirable than the prior reaction, Because of high impurities go along with the product. However, ^{165}Er production via $^{166}\text{Er}(p,2n)^{165}\text{Tm} \rightarrow ^{165}\text{Er}$ reaction lead to high cross section for ^{165}Tm , but this reaction can not be resulted in no-carrier added of ^{165}Er production. $^{165}\text{Ho}(p,n)^{165}\text{Er}$ is suggested as the best method to produce ^{165}Er , generating minimum impurities. Moreover, its non-carrier added production feasibility using proton energy of less 9 MeV can be considered as a brilliant advantage. Solvent extraction (by HDEHP (di-(2-ethylhexyl) phosphoric acid); H_3Cit (citric acid); HLact (lactic acid) and HGlyc (glycolic acid) and ion exchange chromatography are the best method which used for separation erbium radionuclides from Ho targets solution.

5. References

- [1] A. I. Kassis, "Cancer Therapy with Auger Electrons: Are We Almost There?" *Journal of Nuclear Medicine*, Vol. 44, No. 9, 2003, pp.1479-1481.
- [2] J. L. Humm, R. W. Howell and D. V. Rao, "Dosimetry of Auger-Electron-Emitting Radionuclides, Report No. 3 of AAPM Nuclear Medicine, Task Group No. 6," *Medical Physics*, Vol. 21, No. 12, 1994, pp. 1901-1915.
- [3] R. W. Howell, V. R. Narra, K. S. Sastry and D. V. Rao,

- “Auger Electron Dosimetry, Report No. 37 of AAPM Nuclear Medicine, Task Group No. 2,” *Medical Physics*, Vol. 19, No. 16, 1992, pp. 1352-1383.
- [4] H. Thisgaard, “Accelerator Based Production of Auger-Electron Emitting Isotopes for Radionuclide Therapy,” Denmark, Risø-PhD-42(EN), 2008, pp. 2-6.
- [5] A. Bishayee, D. V. Rao and R. W. Howell, “Radiation Protection by Cysteamine Against the Lethal Effects of Intracellularly Localized Auger Electron, α -, and β -Particle Emitting Radionuclides,” *Acta Oncology*, Vol. 39, No. 6, 2000, pp. 713-717.
- [6] A. Bishayee, H. Z. Hill, D. Stein, D. V. Rao and R. W. Howell, “Free Radical-Initiated and Gap Junction-Mediated Bystander Effect Due to Non-Uniform Distribution of Incorporated Radioactivity in a Three-Dimensional Tissue Culture Model,” *Radiation Research*, Vol. 155, No. 2, 2001, pp. 335-344.
- [7] A. Kassis and S. J. Adelstein, “Radiobiologic Principles in Radionuclide Therapy,” *Nuclear Medicine*, Vol. 46, No. 1, 2005, pp. 4S-12S.
- [8] A. Kassis, “Therapeutic Radionuclides: Biophysical and Radiobiologic Principles,” *Seminars in Nuclear Medicine*, Vol. 38, No. 5, 2008, pp. 358-366.
- [9] M. Blann, “ALICE-91, Statistical Model Code System with Fission Competition, RSIC Code,” PACKAGE PSR-146, 1991.
- [10] A. Yu. Konobeyev, Yu. A. Korovin and P. E. Pereslavtsev, “Code ALICE/ASH for Calculation of Excitation Functions, Energy and Angular Distributions of Emitted Particles in Nuclear Reactions,” Report of the Obninsk Institute of Nuclear Power Engineering, 1997.
- [11] Yu. A. Korovin, A. Yu. Konobeyev, P. E. Pereslavtsev, C. Broeders, I. Broeders, U. Fischer and U. von Möllendorff, “Evaluated Nuclear Data Files for Accelerator Driven Systems and Other Intermediate and High-Energy Applications,” *Nuclear Instruments and Methods in Physics Research, Section A*, Vol. 463, No. 3, 2001, pp. 544-556.
- [12] C. H. M. Broeders, A. Yu. Konobeyev and Yu. A. Korovin, “ALICE/ASH-Pre-Compound and Evaporation Model Code System for Calculation of Excitation Functions, Energy and Angular Distributions of Emitted Particles in Nuclear Reactions at Intermediate Energies,” Forschungszentrum Karlsruhe GmbH, Karlsruhe, Report FZKA 2006. <http://bibliothek.fzk.de/zb/berichte/FZKA7183.pdf>
- [13] C. H. M. Broeders and A. Yu. Konobeyev, “Phenomenological Model for Non-Equilibrium Deuteron Emission in Nucleon Induced Reaction,” *Kerntechnik*, Vol. 70, No. 5-6, 2005, pp. 260-269.
- [14] A. Iwamoto and K. Harada, “Mechanism of Cluster Emission in Nucleon,” *Physical Review C-Nuclear Physics*, Vol. 26, No. 5, 1982, pp. 1821-1834.
- [15] M. Blann, “Hybrid Model for Pre-equilibrium Decay in Nuclear Reactions,” *Physical Review Letters*, Vol. 27, No. 6, 1971, pp. 337-340.
- [16] E. Beták and J. Dobeš, “The Finite Depth of the Nuclear Potential Well in the Exciton Model of Preequilibrium Decay,” *Zeitschrift für Physik A: Atoms and Nuclei*, Vol. 279, No. 3, 1976, pp. 319-324.
- [17] C. Kalbach, “Surface and Collective Effects in Preequilibrium Reactions,” *Physical Review C-Nuclear Physics*, Vol. 62, No. 4, 2000, pp. 446081-4460814.
- [18] C. Kalbach, “Erratum: Surface and Collective Effects in Preequilibrium Reactions,” *Physical Review C-Nuclear Physics*, Vol. 64, No. 3, 2001, p. 39901(E).
- [19] C. Kalbach, “Surface Effects in Pre-equilibrium Reactions of Incident Neutrons,” *Physical Review C-Nuclear Physics*, Vol. 69, No. 1, 2004, p. 14605.
- [20] K. Sato, A. Iwamoto and K. Harada, “Pre-equilibrium Emission of Light Composite Particles in the Framework of the Exciton Model,” *Physical Review C*, Vol. 28, No. 4, 1983, pp. 1527-1537.
- [21] A. Yu. Konobeyev and Yu. A. Korovin, “Calculation of Deuteron Spectra for Nucleon Induced Reactions on the Basis of the Hybrid Exciton Model Taking into Account Direct Processes,” *Kerntechnik*, Vol. 61, No. 1, 1996, pp. 45-49.
- [22] T. Belgya, O. Bersillon, T. Fukahori *et al.*, “Handbook for Calculations of Nuclear Reaction Data,” IAEA-TEC-DOC-1506, Vienna, Austria, 2006.
- [23] A. J. Koning, S. Hilaire and M. Duijvestijn, “TALYS-1.2 A Nuclear Reaction Program, User Manual,” NRG, Netherlands, 2009, pp. 16-18.
- [24] V. F. Weisskopf and D. H. Ewing, “Excitation of Nuclei by Bombardment with Charged Particles,” *Physical Review*, Vol. 57, No. 12, 1940, pp. 472-485.
- [25] A. V. Ignatyuk, K. K. Istekov and G. N. Smirenkin, “The Role of Collective Effects in the Systematics of Nuclear Level Densities,” *Yadernaya Fizika*, Vol. 29, No. 4, 1979, pp. 875-883.
- [26] H. Büyüksulu, A. Kaplan, E. Tel, A. Aydın, G. Yıldırım and M. H. Bölükdemir, “Theoretical Cross Sections of ^{209}Bi , ^{232}Th , ^{235}U and ^{238}U on Deuteron-Induced Reactions,” *Annals of Nuclear Energy*, Vol. 37, No. 4, 2010, pp. 534-539.
- [27] G. J. Beyer, S. K. Zeisler and D. W. Becker, “The Auger-electron Emitter Er-165: Excitation Function of the Ho-165(p,n)Er-165 Process,” *Radiochimica Acta*, Vol. 92, No. 4-6, 2004, pp. 219-223.
- [28] F. Tárkányi, A. Hermanne, S. Takacs, F. Ditrói, B. Király *et al.*, “Experimental Study of the $^{165}\text{Ho}(p,n)$ Nuclear Reaction for Production of the Therapeutic Radioisotope ^{165}Er ,” *Nuclear Instruments and Methods in Physics Research, Section B*, Vol. 266, No. 15, 2008, pp. 3346-3352.
- [29] F. Tárkányi, F. S. Takacs, A. Hermanne, F. Ditrói, “Experimental Study of the $^{165}\text{Ho}(d,2n)$ and $^{165}\text{Ho}(d,p)$ Nuclear Reactions up to 20 MeV for Production of the Therapeutic Radioisotopes ^{165}Er and ^{166g}Ho ,” *Nuclear Instruments and Methods in Physics Research, Section B*, Vol. 266, No. 16, 2008, pp. 3529-3534.
- [30] F. Tárkányi, F. S. Takacs, A. Hermanne, F. Ditrói *et al.*, “Investigation of Production of the Therapeutic Radioisotope ^{165}Er by Proton Induced Reactions on Erbium in

- Comparison with Other Production Routes,” *Applied Radiation and Isotope*, Vol. 67, No. 2, 2009, pp. 243-247.
- [31] J. Ziegler, J. Biersack and U. Littmark, “The Stopping and Range of Ions in Matter, SRIM Code,” USA, 2006. <http://www.srim.org/>
- [32] M. Sadeghi, A. Zali and B. Zeinali, “ ^{86}Y Production via $^{86}\text{Sr}(p,n)$ for PET Imaging at a Cyclotron,” *Applied Radiation and Isotope*, Vol. 67, No. 7-8, 2009, pp. 1393-1396.